ACOUSTICS 2012

Numerical simulation of turbulence interaction noise applied to a serrated airfoil

V. Clair, C. Polacsek, G. Reboul and T. Le Garrec

Onera, Département de Simulation Numérique des Ecoulements et Aéroacoustique, BP 72 - 29, avenue de la Division Leclerc, 92322 Chatillon Cedex
vincent.clair@onera.fr

Turbulent wakes generated by turbofan blades and interacting with the outlet guide vanes are known to be mainly contributing to broadband noise emission of aero-engines at approach conditions. Analytical approaches, such as the well-known Amiet's model can be adopted to estimate the noise generated by turbulent flows impacting thin airfoils, but they are limited by the flat-plate assumptions. The development of numerical methods allowing more complex geometries and realistic flows is required. The method, described in the present paper, is based on a CAA code solving the nonlinear Euler equations. The upstream turbulence is synthesized from a stochastic model and injected into the computational domain through an adapted boundary condition. It is first validated in 2D and 3D against academic flat plate configurations by comparison with Amiet solutions (exact in such cases). Then, 3D computations are applied to simulate the effect of a passive treatment (leading edge serrations) aiming at reducing turbulence interaction noise of an isolated airfoil studied in the framework of European project FLOCON. First calculations on baseline conditions are shown to be able to reproduce the measured spectra and far-field directivities, and the acoustic performances of the serrations (3-4 dB PWL reduction) are fairly well assessed too.

1 Introduction

The prediction and the reduction of broadband noise component due the interaction between the turbulent wake of the fan and the OGV (outlet guide vanes) is an important issue for engine manufacturers. Analytical approaches [1] can be used to estimate the noise resulting from turbulent flows impacting thin airfoils, but they are limited by several assumptions on the geometries. Numerical methods become a necessary way to study complex geometries and realistic flows. Since a full 3D turbofan rotor-stator computation is out of reach, turbulent sources are generally studied through simplified configurations for which high fidelity numerical simulations can be investigated. The gust-airfoil interaction problem has been extensively investigated [2,3,4], and more recently extended to turbulent source problem by means of different stochastic models to be coupled to CAA [5,6].

In the FLOCON project, devoted to turbofan broadband noise prediction and reduction, passive treatments aiming at reducing turbulence interaction noise have been studied. A concept based on sinusoidal serrations at the leading edges of a single airfoil have been investigated by ONERA. This concept has been tested in ISVR anechoic open wind tunnel, and high-noise reductions have been obtained for all studied flow speeds [7]. Two numerical methods have also been proposed to compute turbulence-airfoil interaction noise on the baseline and serrated airfoils. The first one, developed by CERFACS is based on a RANS-LES chaining [8]. The second method, described in this paper, is based on a CAA code solving the nonlinear Euler equations. The upstream turbulence is synthesized from a stochastic model and injected into the computational domain through an adapted boundary condition.

2 Method description

2.1 CAA solver

The calculations are performed with the ONERA code sAbrinA.v0 [9]. It solves the full Euler equations in the time domain, and applying a perturbation form that consists in a splitting of the conservative variables into a mean flow and a fluctuating field. These equations are cast in generalized curvilinear coordinates to simulate flows around complex bodies. Such solving is classically conducted with the help of low-dissipative high-order finite differences (6^{th} order spatial derivatives and 10^{th} order filters), and a 3^{rd} order Runge-Kutta time marching scheme. The code features multi-block structured grids and is parallelized using the MPI library.

To perform rotor-stator interaction calculations, efficient boundary conditions are required to allow both hydrodynamic and acoustic outgoing waves to exit the computational domain without reflections. For this purpose Tam and Webb [10] outflow boundary condition are applied. This condition was tested on basic cases and was found to be very efficient without the need of using stretched cells near the outflow boundaries.

The incoming perturbations are injected in the computational domain through the inflow boundary by using the Tam and Webb inflow boundary condition. This boundary condition permits simultaneously the injection of hydrodynamic perturbations, and the exit of outgoing acoustic waves.

These boundary conditions are initially written in spherical coordinates, and a point is chosen in the domain to be the radiation center. But for calculations on a single airfoil with a long span and periodicity conditions in the spanwise direction, a more suited cylindrical formulation has been adopted. Then the radiation center is translated along the span and the boundary conditions are treated as a succession of plans in the spanwise direction.

2.2 Stochastic model

The stochastic model described here is inspired from Kraichnan's theory [11]. It is based on a Fourier-modes decomposition of the incoming turbulent velocity field modeled by a homogeneous isotropic turbulence (HIT) energy spectrum. As done in Amiet's theory, only the upwash velocity component (normal to the airfoil assimilated as a flat plate) is considered with a spatial distribution over streamwise and spanwise wave numbers.

The modes amplitudes are fitted by a Von Karman energy spectrum, defined by two parameters: the turbulence intensity T_I, and the integral length scale Λ. As done in Casper and Farassat work [12], 3D calculations are performed using the two-wavenumbers spectrum $\Phi_{ww}(k_x,k_y)$ corresponding to the integration of the three-dimensional energy spectrum over the normal wave number k_z. In the same way, for 2D calculations the spectrum is

integrated along the spanwise wave number k_y to obtain the one-wavenumber spectrum $\Phi_{ww}(k_x)$ as used in [5]. The incoming velocity disturbances can be written as:

$$u'(\boldsymbol{x},t)=v'(\boldsymbol{x},t)=0$$

$$w'(\boldsymbol{x},t)=\sum_{i=1}^{N}\sum_{j=1}^{M}2\sqrt{\Phi_{ww}(k_{x,i},k_{y,j})\Delta k_x \Delta k_y}\cos(k_{x,i}x+k_{y,j}y-\omega_i t+\varphi_{i,j}) \quad \text{in 3D (1)}$$

$$w'(\boldsymbol{x},t)=\sum_{i=1}^{N}2\sqrt{\Phi_{ww}(k_{x,i})\Delta k_x}\cos(k_{x,i}x+\omega_i t+\varphi_i) \quad \text{in 2D (2)}$$

where φ is a random phase chosen between 0 and 2π. The unsteady disturbance field is assumed convected through a uniform mean flow in the axial direction (Taylor's frozen turbulence hypothesis), so that the pulsation ω_i is related to the axial wavenumber by $\omega_i=k_{x,i}U_\infty$. The fluctuating velocity field so obtained is divergence-free, which is mandatory to avoid spurious sound sources.

2.3 Far-field radiation

The radiated acoustic field can be directly assessed by the Euler computation, and extrapolation to the far-field is possible if the computation domain is large enough to apply simple spherical spreading corrections or to couple with Kirchhoff of FWH (Ffowcs-Williams and Hawkings) porous surface formulations. Practically, direct CAA solution can be supplemented by integral methods allowing us to limit the size of the mesh, particularly for 3D cases with complex geometries.

Turbulence-airfoil interaction mechanism is known to create dipole sources distributed over the airfoil surface. Thus, far-field radiation can be calculated using standard (solid surface) FWH method, restricted to the loading noise term as in Curle's theory. A frequency domain approach is adopted here, which can be written as:

$$\hat{p}(\boldsymbol{x},\omega)=\int_S \hat{p}(\boldsymbol{y},\omega)n_i.\frac{\partial \hat{G}(\boldsymbol{x},\omega|\boldsymbol{y})}{\partial y_i}dS \qquad (3)$$

where $\boldsymbol{x}$ is the observation position and $\boldsymbol{y}$ is the source position. $\hat{G}(\boldsymbol{x},\omega|\boldsymbol{y})$ is the free field Green's function with uniform flow convection, and $p(\boldsymbol{y},\omega)$ are the wall pressure fluctuations provided by sAbrinA.v0.

3 Validation cases

3.1 Single harmonic gust interacting with a 2D flat plate

These first test cases related to single gust interactions are useful to check the accuracy of the boundary conditions and to highlight specific behaviors such as the compactness effects on the acoustic response for high frequencies. The flat plate case is of particular interest, because exact Amiet solution [1] can used as a reference.

In the following cases, the gust injected only have an axial wavenumber k_x (nondimensionalized by half the chord), and amplitude is chosen to verify the linear domain assumptions (Golubev [3,4] has shown that for high amplitudes gusts, nonlinear effects are responsible of the generation of higher harmonics in the acoustic response). The incident perturbation field is of the form :

$$u'(\boldsymbol{x},t)=0$$

$$w'(\boldsymbol{x},t)=\varepsilon U_0\cos\left(\frac{2k_x}{c}(x-U_0 t)\right) \qquad (4)$$

where c is the chord of the flat plate, $\varepsilon=0.02$ is the gust intensity relative to the mean flow U_0 with a Mach number set to $M=0.5$.

Three grids have been designed in order to ensure at least 10 points per wavelength respectively for the reduced wave numbers $k_x=1$, $k_x=3$ and $k_x=10$. The grids extend at least until 6 chords around the airfoil, and they are clustered at the leading and trailing edges to support the abrupt transition effects and to well capture the pressure peak at the leading edge. In order to speed up the transitional state induced at the beginning of the calculations (before reaching the periodic state), the fluctuating field given by Eq. (4) is initialized over the entire domain.

Fig. 1 shows the RMS pressure on the suction side of the plate and Fig. 2 presents the directivity in the mid plane for an observer radius of 4 chords. As the acoustic responses are symmetric, only the upper half is represented. These results show an expected dipolar radiated field, and the RMS wall pressure as well as the directivities are in good agreement with Amiet's solution. The compactness effects when increasing the reduced frequencies give rise to multi-lobes in the directivity patterns, which are fairly well assessed by the CAA.

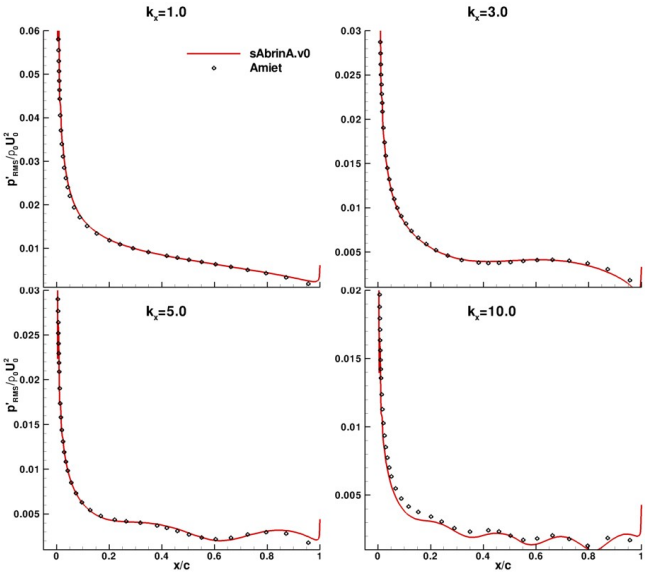

Figure 1: RMS wall pressure for k_x =1, 2, 5 and 10

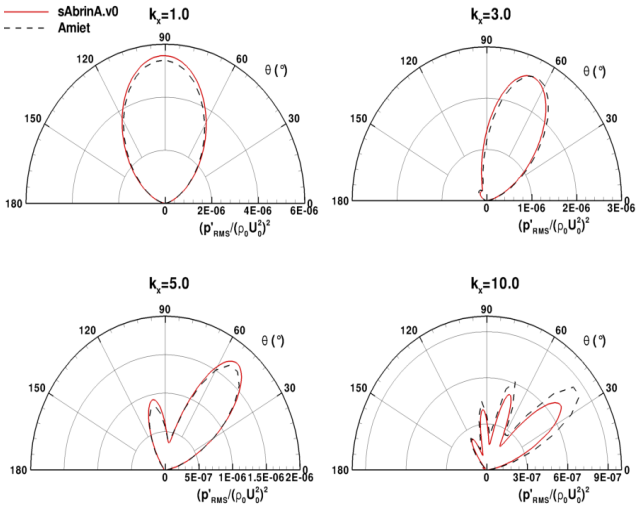

Figure 2: Directivities at 4 chords for k_x =1, 2, 5 and 10

3.2 HIT interacting with a 2D flat plate

The previous flat plate cases are now extended to the computation of a synthetic turbulence described by Eq. (2). The finest mesh (designed for $k_x=10$) is considered and the axial mean flow Mach number is set to $M=0.5$. Modes are injected between $k_{min}=1$ and $k_{max}=10$ with $\Delta k=0.2$. 1D Von Karman spectrum is defined by:

$$\Lambda=0.18m \text{ and } T_I=4.56\times10^{-3}$$

Snapshots of velocity and pressure disturbances computed by CAA are plotted in Fig. 3, clearly showing the symmetric dipolar pattern. Fig. 4 presents the PSD (power spectral density) directly assessed for an observer located at 4 chords above the center of the airfoil and compared to Amiet solution. A very good agreement is observed between the numerical and analytical predictions.

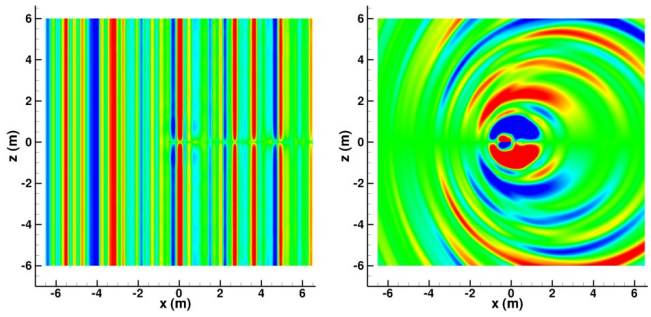

Figure 3: Upwash velocity component (left, ±1m/s) and fluctuating pressure field (right, ±15Pa)

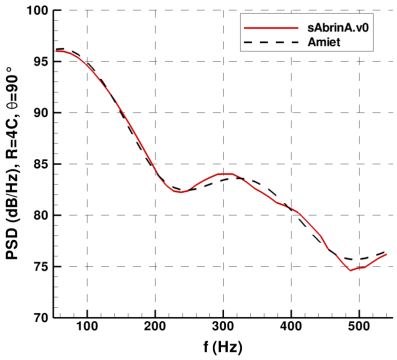

Figure 4: PSD at 4 chords and 90°

3.3 3D flat plate computations and coupling with FWH integral method

The CAA computations are extended in 3D and tested again on the flat plate. The acoustic predictions issued from the coupling with FWH integral described in section 2.3 are presented and discussed.

In order to get a reasonable CAA grid size 3D computations are practically performed by restricting the full span L_{span} to a radial strip with length L_{sim}, and imposing periodicity conditions at each side. This implies to choose wavelengths of spanwise wavenumbers k_y to be multiples of the simulated span ($k_{y,n}=n2\pi/L_{\text{sim}}$), so that the two-wavenumber spectrum $\Phi_{ww}(k_x,k_y)$ is inherently truncated. It appears that the suited spanwise extent required to ensure a significant part of the spectrum related to the most energetic values of k_y (first cut-on oblique gusts) is still demanding heavy mesh size (about 100 Million points), involving quite expensive calculations. As done in [12], a simplification is proposed to avoid this problem.

Amiet argued that for a far-field observer in the mid-span plane of an infinite flat-plate (practically when the span to chord ratio is greater or equal to 3), the parallel gusts ($k_y=0$) are mainly contributing to the radiated noise. Indeed, it can be shown that the contribution of cut-on oblique gusts corresponding to $k_y<k_xM/\sqrt{1-M^2}$ are giving rise to balancing terms getting fully cancelled in the mid-span plane for a far-field observer [13].

Following this observation, only the parallel gusts can be considered in Eq. (1) when injected in the CAA, if the span to chord ratio assumptions are satisfied. However, when using the zero-spanwise wavenumber spectrum $\Phi_{ww}(k_x,0)$, explicit values for Δk_y are no more defined. In Amiet theory, 3D non-compact and 2D compact formulations respectively related to the overall spectrum $\Phi_{ww}(k_x,k_y)$ and to parallel gusts spectrum $\Phi_{ww}(k_x,0)$ give rise to a factor equal to $2\pi/L_{\text{span}}$ when calculating the far-field PSD. This factor has to be also included in the CAA in order to get the correct aerodynamic response of the full span airfoil. This is done by setting $\Delta k_y=2\pi/L_{\text{span}}$.

To check this scaling factor, we consider a flat-plate with $c=0.15\text{m}$ chord and $L_{\text{span}}=0.45m$, and a uniform mean flow $U_o=60m/s$. The Von Karman spectrum is defined with Λ = 6 mm and T_I = 2.5%. These conditions are similar to FLOCON application case presented in section 4. The incoming synthetic turbulence defined by Eq. (1) is restricted to parallel gusts with wavenumbers corresponding to a maximum spectrum frequency $f_{max}=5000\,Hz$ and a frequency spacing $\Delta f=100\,Hz$. The CAA strip is set equal to $L_{\text{sim}}=10\,mm$. Note that in order to take into account for compactness effects, the input data will be duplicated in the spanwise direction over the full span L_{span} before calculating to the FWH integral.

In addition to standard Amiet solutions derived from far-field approximations, a more confident semi-analytical calculation is addressed too, consisting in a FWH (numerical) integration of the pressure jump over the plate computed using Amiet-based aerodynamic function. Thus, the actual acoustic response including oblique cut-on modes contribution with full compactness effects (no far-field approximations) can be assessed and compared to the CAA prediction.

A comparison of RMS wall pressure distribution issued from CAA and Amiet-based response is presented in Fig. 5, showing a perfect agreement. A snapshot of the fluctuating pressure issued from direct CAA computation in the mid-span plane is shown in Fig. 6. The possibility of using the direct acoustic pressure field to estimate the far-field PSD with suited scaling factors has been investigated, but absolute levels so obtained are doubtful so that we only focus here on the CAA-FWH approach. Fig. 7 presents the results for a 90° observer point located in the mid-span plane at 1.2 m and 90° over the airfoil. The computed PSD provided by CAA-FWH is closed to Amiet-based solutions obtained with and without including the oblique gusts.

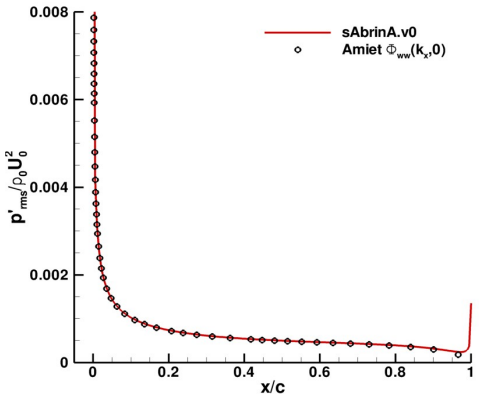

Figure 5: RMS wall pressure for the 3D flat plate

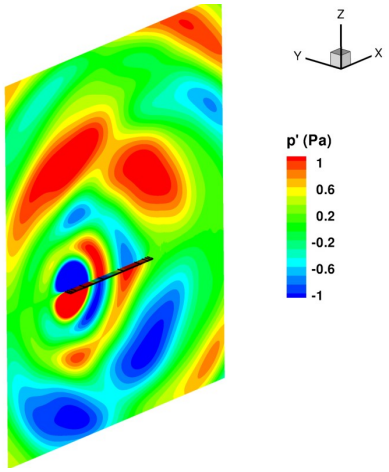

Figure 6: Snapshot of disturbance pressure field in the mid-span plane

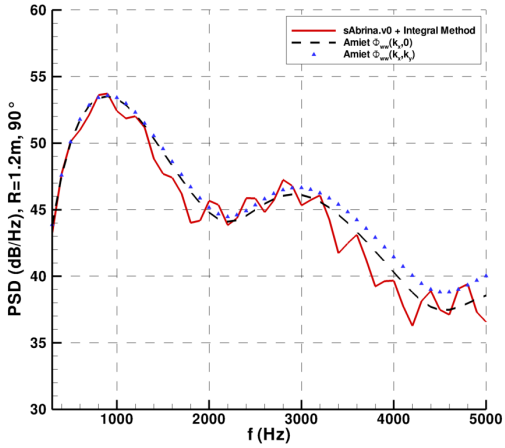

Figure 7: Predicted PSD at R_{obs} = 1.2 m and 90°

4 Application to FLOCON configuration and simulations of leading edge serration effect

The methodology described in Sec. 1 is now applied in the frame of the European project FLOCON on both a baseline configuration (untreated NACA651210) and a serrated leading edge configuration. The tests performed at ISVR have shown significant broadband noise reductions on a wide frequency range for all studied flows [7].

The airfoils have a 0.15 m chord and a 0.45 m span. The spanwise extent of the CAA domain is set equal to $L_{sim}=10\,mm$ (as done previously) and the mean flow is assumed to be fully uniform ($U_o=60\,m/s$). The synthetic turbulent field injected in the computational domain is the same than in Sec. 3.3 too. The mesh for the baseline configuration consists in approximately 8.5 millions of grid points, and the calculation time is around 120 hours on 256 SGI Altix processors. As for the flat plate test case, the extracted unsteady data are duplicated in the spanwise direction to reach the actual 0.45 m span.

Fig. 8 presents the PSD obtained for the baseline configuration for the observer at 90° and 1.2 m over the airfoil (corresponding to a microphone position of ISVR test rig). It is compared to the experiment and to an Amiet solution (already plotted in Fig. 7). Despite of a noticeable deviation on the peak level and for low frequencies behind 1 kHz, the agreement is quite satisfactory. Note that numerical predictions are very close to Amiet solution which is consistent with preliminary 2D computation results. As shown in [7,8], a better agreement should be obtained if a more representative convection effects (RANS mean flow solution) was considered in the CAA, since the presence of shear layers tend to increase the attenuation slope of the acoustic spectrum.

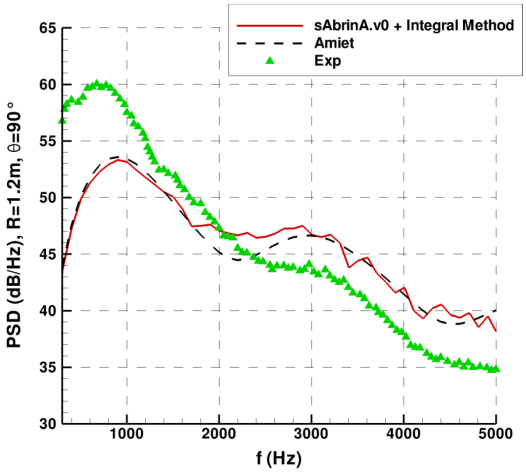

Figure 8: PSD at R_{obs}= 1.2m and 90° for the baseline case

The serrated airfoil calculation requires a finer discretisation in the spanwise direction, leading to an approximately 13.5 millions of grid points mesh. The calculation time is around 300 hours on 256 processors. A partial view of the CAA grid is presented in Fig. 9. The 10 mm strip is equal to the wavelentgh of the serrations.

Fig. 10 shows a PSD comparison between the baseline and the serrated configurations issued from the experiment (Fig. 10 left) and the computations (Fig. 10 right). Similar trends are visible between the measurements and the numerical predictions with very close level reductions up to 3,5 kHz. Beyond, the PWL attenuation due to the serrations is over-estimated by the simulations. It might be due to the fact that oblique gusts ($k_y \neq 0$) contribution, not taken into account here, is no more cancelling at these frequencies (contrarily to the straight leading edge case). As a consequence, it could tend to balance the overall level as the parallel gusts are getting almost fully cut-off at higher frequencies.

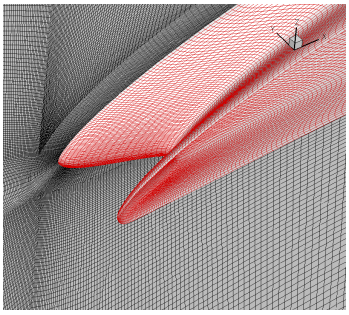

Figure 9: Partial view of the mesh for the serrated airfoil

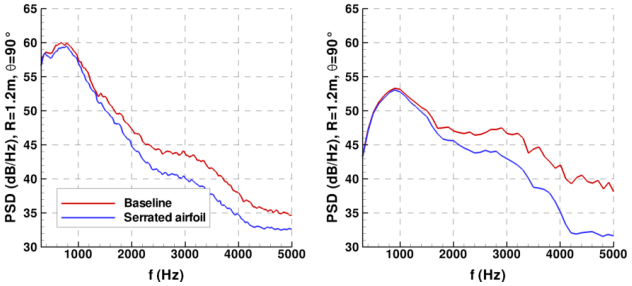

Figure 10: PSD comparison between baseline and serrated airfoil. Experiment (left) and numerical predictions (right)

5 Conclusion

A CAA Euler based method aiming at predicting turbulence interaction noise has been presented. It has been validated on two dimensional cases against analytical model results, and the coupling with an integral method has been validated for a three dimensional flat plate and considering only parallel gusts. The method has then been applied to an isolated 3D airfoil impacted by an isotropic turbulent flow, in the frame of the European project FLOCON, in order to assess the effect of leading edge serrations on the radiated field. The acoustic spectra and noise reduction provided by experiment have been fairly well reproduced by the present simulations, although uniform mean flow approximation has been used. However, the contribution of the oblique gusts (discarded here) is probably required in order to simulate accurately the acoustic response of the serrations at high frequencies. An additional computation using a larger spanwise domain extent aiming to simulate a reliable two-wavenumber turbulence spectrum should be performed soon in order to status about this point.

Acknowledgments

This work was supported by the European Commission (FLOCON). Authors would like to thank Mat Gruber (ISVR) for having performing and providing the experimental data.

References

[1] R.K. Amiet, “Acoustic radiation from an airfoil in a turbulent stream”, *J. Sound Vib.* 41, 407-420 (1975)

[2] J.R. Scott, “Single airfoil gust response problem”, *4th CAA Workshop on Benchmark Problems*, NASA CP-2004-212954, 45-58 (2003)

[3] V.V. Golubev, R.R. Mankbadi, J.R. Scott, “Numerical inviscid analysis of nonlinear airfoil response to impinging high-intensity gust”, *10th AIAA/CEAS Aeroacoustics Conf.*, AIAA-2004-3002 (2004)

[4] V.V. Golubev, R.R. Mankbadi, M.R. Visbal, J.R. Scott, R. Hixon,”A parametric study of nonlinear gust-airfoil interaction”, *12th AIAA/CEAS Aeroacoust. Conf.*, AIAA-2006-2426 (2006)

[5] M. Dieste, G. Gabard, “Synthetic turbulence applied to broadband interaction noise”, *15th AIAA/CEAS Aeroacoustics Conf.*, AIAA-2009-3267 (2009)

[6] A.H. Salem-Said, Large eddy simulation of shear-free interaction of homogeneous turbulence with a flat-plate cascade, PhD Thesis, Virginia Polytechnic Institute and State Univ. (2007)

[7] C. Polacsek, G. Reboul, V. Clair, T. Le Garrec, H. Deniau, “Turbulence-airfoil interaction noise reduction sing wavy leading edge: an experimental and numerical study”, *Internoise Conf. 2011* (2011)

[8] H. Deniau, G. Dufour, J.F. Boussuge, C. Polacsek, S. Moreau, “Affordable compressible LES of airfoil-turbulence interaction in a free jet”, *17th AIAA/CEAS Aeroacoustics Conf.*, AIAA-2011-2707 (2011)

[9] S. Redonnet, E. Manoha, P. Sagaut, “Numerical simulations of propagation of small perturbations interacting with flows and solid bodies”, *7th AIAA/CEAS Aeroacoustics Conf.*, AIAA-2001-222 (2001)

[10] C.K.W. Tam, “Advances in numerical boundary conditions for computational aeroacoustics”, *J. Comp. Acoust.* 6, 377-402 (1998)

[11] R.H. Kraichnan, “Diffusion by a random velocity field”, *Physics of fluids* 13(1), 22-31 (1970)

[12] J. Casper, F. Farassat, “A new time domain formulation for broadband noise predictions”, *Int. J. of Aeroacoust.* 1(3), 207-240 (2002)

[13] J.M.R. Graham,”Similarity rules for thin aerofoils in non-stationary subsonic flows”, *J. Fluid Mech.* 43(4), 753-766 (1970)